RAPID COMMUNICATIONS

PHYSICAL REVIEW E VOLUME 48, NUMBER 2 AUGUST 1993

Scaling behavior of self-avoiding tethered vesicles

Z. Zhang and H. T. Davis*
Department of Chemical Engineering and Materials Science and Center for Interfacial Engineering, University of Minnesota, Minneapolis, Minnesota 55455

D. M. Kroll
Institut für Festkörperforschung, KFA Jülich, Postfach 1913, 5170 Jülich, Germany
(Received 5 March 1993)

The scaling behavior of self-avoiding tethered vesicles is analyzed using shell theory and scaling arguments. For closed networks, there is a linear coupling between the out-of-plane undulation modes and the in-plane phonon modes that causes a strong suppression of out-of-plane fluctuations at long length scales. This leads to new scaling behavior, which has important consequences for the analysis of experimental and simulation data. Molecular-dynamics simulation data for tethered vesicles are also presented and analyzed using these results. We find that the exponent η, which describes the scale dependence of the bending rigidity, has the value $\eta = 0.81 \pm 0.03$.

PACS number(s): 82.65.Dp, 05.40.+j, 87.10.+e

Tethered surfaces are idealized models of flexible two-dimensional solid sheets or molecular networks that are free to fluctuate in three-dimensional space. These surfaces have a finite shear modulus so that the statistical mechanics of tethered networks is controlled by a delicate interplay between the in-plane elastic modes and the out-of-plane undulation modes. Two realizations of these objects that have recently attracted a great deal of attention are exfoliated graphite oxide crystals [1] and the spectrin network of mammalian red blood cells [2–4].

Mammalian red blood cells consist of a multilayered membrane structure made up of a cross-linked network of proteins — the cytoskeleton — that lines the cytoplasm side of the (liquid) lipid bilayer cell membrane. The cytoskeleton provides a shear elasticity that prevents membrane loss during large deformations induced by flow in the cardiovascular system. Understanding the statistical thermodynamics of this polyelectrolytic network is a crucial step in determining the properties of the composite membrane, and ultimately, its role in the function of red blood cells.

The lipids of the cell membrane can be dissolved by detergent treatment, leaving behind an extracted membrane skeleton. Freshly isolated skeletons are very flexible, roughly spherical shells. With a combination of light and synchrotron-based small-angle x-ray scattering it has been possible to characterize the extracted cytoskeleton network and measure its static structure factor over four orders of magnitude in length scale, thus providing the best currently available experimental data on well characterized tethered networks [2–4]. In particular, these experiments support simulation results [4–7] that indicate that self-avoiding tethered networks are in a "flat phase" in which the rms amplitude of the out-of-plane fluctuations scale with the in-plane length scale with a power less than 1.

An analysis of the elastic Hamiltonian for zero mean curvature tethered networks shows that in this phase, the bending rigidity κ diverges at large length scales, whereas the in-plane elastic shear and compressional moduli soften to zero [8,9]. The renormalization of the elastic constants arises from nonlinear couplings between the out-of-plane undulation modes and the in-plane phonon modes. The stretching that accompanies the bending of a tethered network of zero mean curvature is a second-order effect in the out-of-plane displacement. In a harmonic approximation, the out-of-plane undulation modes remain eigenmodes of the system at all length scales.

The situation is entirely different for closed networks; in this case, dilatation or shear is a first-order effect, and, for example, a spherical shell or tethered vesicle cannot bend without being stretched. This property is most easily seen by considering the uniform stretching of a spherical shell [10]. If every point of the sheet undergoes the same radial displacement w, the length of the equator increases by $2\pi w$ so that the strain tensor is proportional to the first power of w. This very general property of nonplanar closed shells has been known for over a century [11,12]. Its consequences for the scaling behavior of closed tethered networks, such as the red blood cell cytoskeletons studied in [2–4], do not, however, appear to have been appreciated [13–15]. In this paper we explore the consequences of this fact and present the results of an analysis of the scaling behavior of self-avoiding tethered vesicles. We consider a flaccid tethered sphere, which is the simplest case to analyze; the results, however, remain valid also in more general cases, such as when there are constraints on the enclosed volume or surface area of the vesicle. Molecular-dynamics simulation data for the equilibrium structure of closed self-avoiding tethered vesicles are also presented and analyzed using these results. We find, in particular, that the exponent η that describes the scale dependence of the bending rigidity has the value $\eta = 0.81 \pm 0.03$. This result for η is somewhat larger than earlier estimates for open membranes with free edge boundary conditions, but is in excellent agreement with the value obtained using a self-consistent screening approximation [16].

For a closed, homogeneous surface, the elastic bending

energy F_b is given by the Helfrich Hamiltonian [17]

$$F_b = \frac{\kappa}{2}\int dS\ (K_\alpha^\alpha - c_0)^2, \tag{1}$$

where dS is an element of area on the surface, κ is the bending rigidity, K_α^α is the trace of the curvature tensor (repeated indices are summed over), and c_0 is the spontaneous curvature. Here we assume that c_0 is a constant equal to $2/R$, where R is the average radius of the spherical vesicle. In this case [12],

$$K_\beta^\alpha = \delta_\beta^\alpha/R + D^\alpha D_\beta w + \delta_\beta^\alpha w/R^2 \tag{2}$$

to lowest order in the deformation, where D_α (D^α) denote the two-dimensional covariant (contravariant) derivatives in the internal coordinates of the surface and w is a scalar field representing the radial displacements. The dilatation and shear energy are given by [10,12]

$$F_e = \int dS\left[\mu E_\alpha^\beta E_\beta^\alpha + \frac{\lambda}{2}(E_\alpha^\alpha)^2\right], \tag{3}$$

where, for a sphere, the strain tensor [12]

$$E_\beta^\alpha = \tfrac{1}{2}(D^\alpha v_\beta + D_\beta v^\alpha) + \delta_\beta^\alpha w/R \tag{4}$$

to lowest order. $\mathbf{v}$ is a tangential vector describing the deviation of a surface element of the shell from its zero-temperature equilibrium position, v_α and v^α are the covariant and contravariant components of $\mathbf{v}$, and λ and μ are the Lamé constants of the two-dimensional network. The total free-energy functional to second order in w and $\mathbf{v}$ for the spherical shell is given by $F = F_b + F_e$.

$\mathbf{v}$ can be written as the sum of an irrotational and a solenoidal part as

$$v_\beta = D_\beta \Psi + \gamma_{\gamma\beta} D^\gamma \chi, \tag{5}$$

where Ψ and χ are two scalar functions and $\gamma_{\alpha\beta}$ is the alternating tensor in two dimensions. With the aid of (5), the free energy can be written as $F = F_1[w,\Psi] + F_2[\chi]$, where

$$F_1[w,\Psi] = \int dS\Big\{\frac{\kappa}{2}w(\Delta + 2/R^2)^2 w + \frac{2K}{R^2}w^2 + \frac{2K}{R}w\Delta\Psi + \frac{1}{2}(K+\mu)(\Delta\Psi)^2 + \frac{\mu}{R^2}\Psi(\Delta\Psi)\Big\}, \tag{6}$$

and

$$F_2[\chi] = \int dS\left\{\frac{\mu}{2}\Delta\chi[\Delta\chi + 2\chi/R^2]\right\}; \tag{7}$$

Δ is the two-dimensional Laplacian and $K = \mu + \lambda$ [18]. Note that there is no coupling between $\{w,\Psi\}$ and χ so that the in-plane shear modes are eigenmodes of the system. However, w and the longitudinal part of the in-plane displacement field couple due to the presence of the term $2Kw\Delta\Psi/R$ in (6). This coupling vanishes in the limit $R \to \infty$, as it should.

The dispersion relation for the modes involving w and Ψ can be determined by expanding in the spherical harmonics $Y_l^m(\theta,\phi)$ [19]. Writing $w = \sum_{l,m} A_{lm} R Y_l^m(\theta,\phi)$ and $\Psi = \sum_{l,m} B_{lm} R^2 Y_l^m(\theta,\phi)$, and using $\Delta Y_l^m = -[l(l+1)/R^2]Y_l^m$, F_1 becomes

$$F_1 = \sum_{l,m} R^2\Big\{[\kappa(l-1)^2(l+2)^2/(2R^2) + 2K]A_{lm}^2 - 2Kl(l+1)A_{lm}B_{lm} + \tfrac{1}{2}l(l+1)[(K+\mu)l(l+1) - 2\mu]B_{lm}^2\Big\}. \tag{8}$$

The normal modes of the shell are easily determined from (8). In particular, for the relevant range of system parameters and l greater than 2 or 3, the w-w propagator $\Lambda_w(l) \equiv \langle R^2 A_{lm}^2\rangle^{-1}$ is well approximated by

$$\Lambda_w(l) \approx \kappa(l-1)^2(l+2)^2/R^2 + E, \tag{9}$$

where $E = 4\mu K/(K+\mu)$ is the two-dimensional Young modulus. $\Lambda_w(0) = 4[\kappa/R^2 + K]$, while $\Lambda_w(1) = 0$; this latter mode corresponds to a uniform translation of the spherical surface. The spherical topology therefore leads to an infrared cutoff for the out-of-plane modes. This is due to the curvature induced linear coupling between the undulation modes with the in-plane longitudinal phonon modes. In contrast, the dispersion relation for the longitudinal phonon mode is qualitatively similar to that in a zero mean curvature tethered surface.

For a finite system, the l sum in (8) is cut off at an l_M determined by the requirement that the total number of modes be equal to the number of degrees of freedom. Denoting the number of degrees of freedom by $3N$, this means that $(l_M+1)^2 \simeq N$. For a given system size, the infrared cutoff in (9) is important for l smaller than an l_c such that $(l_c-1)^2(l_c+2)^2 \simeq ER^2/\kappa$. It turns out that $1 < l_c < l_M$ for the sytems of interest. For a thin spherical shell of thickness a and radius R constructed from an isotropic material in three dimensions, one finds [10,15], for example, $\kappa = (\lambda+2\mu)a^2/12$ so that $ER^2/\kappa \sim (R/a)^2 \gg 1$. For a red blood cell, $\kappa \simeq 3\times10^{-20}$ J and $E \simeq 2\times10^{-5}$ J/m^{-2} [15,20–22]. Using an effective radius $R = 1$ μm, one obtains $ER^2/\kappa \simeq 7\times10^2$. Finally, for our simulations to be described below, we estimate that $ER^2/\kappa \simeq 3N$, where N is the number of surface monomers, so that for large N, $l_c \simeq (3N)^{1/4} \simeq \sqrt{l_M}$. Thus in all three cases the coupling between the undulation modes and the in-plane compressional modes will influence the long length-scale fluctuation spectra of the tethered network.

At length scales shorter than $L^* \simeq (R^2\kappa/E)^{1/4}$, the fluctuation spectra of the shell are essentially the same as that of a flat network. At these length scales, κ as well as λ and μ are scale dependent. In particular, the bending rigidity will renormalize according to $\kappa_R(q) \sim \kappa_0 q^{-\eta}$, and $\mu_R(q) \sim \lambda_R(q) \sim q^\omega$, where $q \sim l/R$. The exponents ω and η obey the scaling relation $\omega + 2\eta = 2$ [9]. Renormalization continues until $q \simeq q_c$, where $q_c^4 \simeq E(q_c)/[R^2\kappa(q_c)]$, or, equivalently, $q_c^{2+\eta} \simeq E_0/[\kappa_0 R^2]$. For $q < q_c$, renormalization stops and the elastic constants remain proportional to their values at q_c [23]. Note that if $l_c \simeq l_M$, there will be *no* renormalization of the elastic

constants [23].

Introducing these q-dependent renormalized elastic constants into the Gaussian Hamiltonian corresponding to (8) [24,25], we find, for example, that

$$\chi_v = \sqrt{\langle V^2\rangle - \langle V\rangle^2} \simeq R^2\sqrt{\pi/K(q_c)} \sim R^{6/(2+\eta)} \quad (10)$$

and

$$\chi_g = \sqrt{\langle (R_g^2)^2\rangle - \langle R_g^2\rangle^2} \simeq R/[4\pi K(q_c)]^{1/2} \sim R^{(4-\eta)/(2+\eta)}, \quad (11)$$

where we have assumed that $1 \ll l_c \ll l_M$ (as we expect to be the case in the systems of interest). Similarly,

$$\langle w^2\rangle = \frac{\langle \int dS\, w^2\rangle}{\langle \int dS\rangle} \sim R^{2(2-\eta)/(2+\eta)}. \quad (12)$$

Equation (11) is often used to measure the amplitude of the undulation fluctuations of the vesicle [4,26,27]. The difference between (11) and (12) is due to the fact that the leading contribution to (11) is proportional to $(\langle \int dSw \int dSw\rangle)^{1/2}/R$, so that the contribution from the $l = n = 0$ mode dominates. For a flat tethered network the rms amplitude of the out-of-plane fluctuations $L_\perp$ is related to the in-plane length scale L by $L_\perp \sim L^\zeta$, with $\zeta = 1 - \eta/2$. In contrast, (11) implies $\zeta_1 = (2-\eta/2)/(2+\eta)$, and (12), $\zeta_2 = (2-\eta)/(2+\eta)$.

We have performed extensive molecular-dynamics simulations of closed tethered vesicles containing between $N = 162$ to 1962 monomers utilizing the same heat-bath algorithm and potential parameters as Grest [28]. This model consists of a purely repulsive shifted Lennard-Jones repulsive potential between all monomers as well as a nonharmonic tethering potential between nearest neighbors. In the following, all lengths are measured in units of σ, the length scale appearing in the Lennard-Jones potential. In these units, the average interparticle distance is approximately 0.97. Between 6×10^6 (for $N = 162$) and 19×10^6 (for $N = 1962$) time steps were used for evaluating averages.

Our results for χ_v as well as χ_g are plotted in Fig. 1(a); those for $\langle w^2\rangle$ in Fig. 1(b). There are rather large finite-size effects, due either to the rigidity of our network or the rather small value of the infrared cutoff for small system sizes. Nevertheless, for larger systems, our results are consistent with $\eta = 0.81 \pm 0.03$. This value for η is significantly larger than that obtained from simulations of flat tethered networks, but is consistent with the result $\sqrt{\chi_g} \sim N^{0.56}$ (which implies $\eta \simeq 0.83$) quoted in Refs. [4] and [27]. It also agrees with recent theoretical results described in Ref. [16].

The data can be used to estimate $K(q_c)$ and $\kappa(q_c)$. In particular, the results for χ_g imply $K(q_c) \simeq 45\sigma^{-2}$ for $N = 642$, and this result, together with (12), suggests that $\kappa(q_c) \simeq 6$ for this system size [29]. We estimate the uncertainty in $K(q_c)$ to be on the order of $10-20\,\%$; the estimate for $\kappa(q_c)$ is less accurate.

Finally, in Fig. 2 we present our results for the directionally averaged structure factor $S(q)$ for $N = 642$ and 1962 plotted as a function of $x = qR^{2/(3-\zeta)}$ using

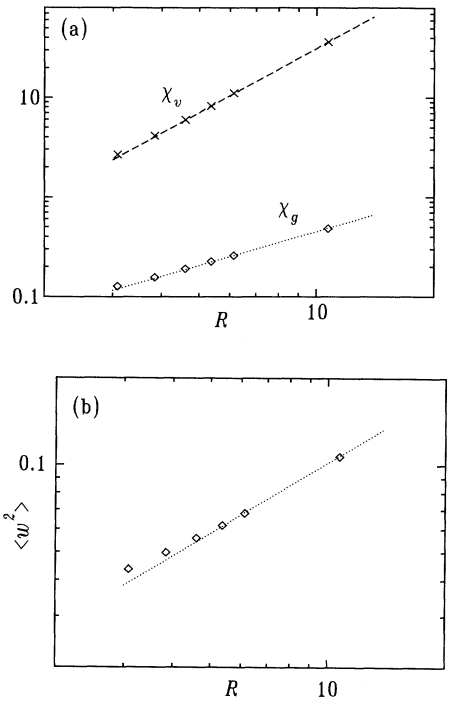

FIG. 1. (a) χ_v ($\times$) and χ_g ($\diamond$) vs $R \equiv \sqrt{R_g^2} \sim \sqrt{N}$ for $N = 162$, 252, 362, 492, 642, and 1962. The dashed line has the slope 2.15 ($\eta = 0.79$), the dotted line, 1.13 ($\eta = 0.82$). (b) $\langle w^2\rangle$ vs R for the same system sizes. The dotted line has the slope 0.81 ($\eta = 0.85$). Due to the large finite-size corrections, this is clearly an overestimate of the true value of η.

$\zeta = 0.6$ (which corresponds to $\eta = 0.8$). The oscillations characteristic of the spherical shell form factor persist to rather large q vectors because of the ideal monodispersity of our network and the small amplitude of fluctuations. We expect [30], in general, that $S(q) \sim 1/x^{3-\zeta}$ for $1/\sigma \gg q \gg q_c$. The solid line is a plot of the expected large-q behavior $x^{-(3-\zeta)}$ for $\zeta = 0.6$. This result is in good agreement with the experimental data of Ref. [4].

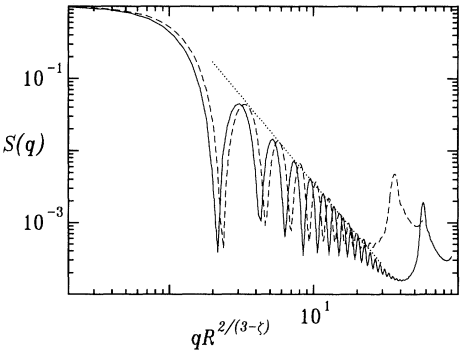

FIG. 2. Directionally averaged structure factor $S(q)$ vs $qR^{2/(3-\zeta)}$ for system sizes $N = 642$ (dashed line) and 1962 (solid line) using $\eta = 0.8$. The dotted line is a plot of $1/(R^2q^{3-\zeta})$ for this same value of η.

We have shown that the linear coupling between out-of-plane undulation modes and in-plane phonon modes in closed tethered surfaces leads to new scaling behavior at large length scales. These results were used to analyze molecular-dynamics data for closed flaccid tethered vesicles. We find that $\eta \simeq 0.8$, a value considerably larger than that obtained in simulation studies of open, flat networks [5-7], but in excellent agreement with the value determined using a self-consistent screening approximation [16].

D.M.K. acknowledges helpful discussions with G. Gompper. This work was supported in part by the U.S. Army Research Office, Contract No. DAAL 03-89-C-0038 with the Army High Performance Computing Research Center at the University of Minnesota.

---

* Present address: Laboratoire de Physique Statistique, L'ecole Normale Superieure, 24, rue L'homond, 75231 Paris Cedex 05, France.

[1] T. Hwa, E. Kokufuta, and E. Tanaka, Phys. Rev. A **44**, 2235 (1991); X. Wen, C.W. Garland, T. Hwa, M. Kardar, E. Kokufuta, Y. Li, M. Orkisz, and T. Tanaka, Nature **355**, 426 (1992).

[2] C.F. Schmidt, K. Svoboda, N. Lei, C.R. Safinya, S.M. Block, and D. Branton, in *The Structure and Conformation of Amphiphilic Membranes*, edited by R. Lipowsky, D. Richter, and K. Kremer, Springer Proceedings in Physics Vol. 66 (Springer-Verlag, Berlin, 1992), p. 128.

[3] K. Szoboda, C.F. Schmidt, D. Branton, and S.M. Block, Biophys. J. **63**, 784 (1992).

[4] C. Schmidt, K. Szoboda, N. Lei, I.B. Petsche, L.E. Berman, C.R. Safinya, and G. Grest, Science **259**, 952 (1993).

[5] M. Plischke and D.H. Boal, Phys. Rev. A **38**, 4943 (1988); F.F. Abraham, W.E. Rudge, and M. Plischke, Phys. Rev. Lett. **62**, 1757 (1989); J.-S. Ho and A. Baumgärtner, *ibid.* **63**, 1324 (1989); D.H. Boal, E. Levinson, D. Liu, and M. Plischke, Phys. Rev. A **40**, 3292 (1989).

[6] G. Gompper and D.M. Kroll, Europhys. Lett. **15**, 783 (1991); J. Phys. I France **1**, 1411 (1991).

[7] F.F. Abraham and M. Goulian, Europhys. Lett. **19**, 293 (1992); D.M. Kroll and G. Gompper, J. Phys. I France **3**, 1131 (1993).

[8] D.R. Nelson and L. Peliti, J. Phys. (Paris) **48**, 1085 (1987).

[9] J.A. Aronovitz and T.C. Lubensky, Phys. Rev. Lett. **60**, 2634 (1988).

[10] L.D. Landau and E.M. Lifshitz, *Theory of Elasticity* (Pergamon, Oxford, 1959).

[11] J.H. Jellet, Roy. Irish Acad. Trans. **22**, 343 (1855).

[12] F.I. Niordson, *Shell Theory* (North-Holland, New York, 1985).

[13] Two exceptions are Refs. [14] and [15].

[14] M.A. Peterson, H. Strey, and E. Sackmann, J. Phys. II France **2**, 1273 (1992).

[15] S. Komura and R. Lipowsky, J. Phys. II France **2**, 1563 (1992).

[16] P. Le Doussal and L. Radzihovsky, Phys. Rev. Lett. **69**, 1209 (1992).

[17] W. Helfrich, Z. Naturforsch. **28C**, 693 (1973).

[18] There are no edge contributions to F because of the spherical topology.

[19] We choose the normalization $\int_S d\Omega\ (Y_l^m)^2 = 1$.

[20] A. Zilker, H. Engelhardt, and E. Sackmann, J. Phys. (Paris) **48**, 2139 (1987).

[21] R. Waugh and E.A. Evans, Biophys. J. **26**, 115 (1979).

[22] H. Engelhardt and E. Sackmann, Biophys. J. **54**, 495 (1988).

[23] There will still be logarithmic corrections; we ignore these effects here.

[24] R. Lipowsky, Europhys. Lett. **7**, 255 (1988).

[25] F.F. Abraham and D.R. Nelson, Science **249**, 4393 (1990); J. Phys. (Paris) **51**, 2653 (1990).

[26] S. Komura and A. Baumgärtner, Phys. Rev. A**44**, 3511 (1991).

[27] I.B. Petsche and G.S. Grest (unpublished).

[28] G.S. Grest, J. Phys. I France **1**, 1695 (1991).

[29] The factor k_BT has been absorbed in our definition of the elastic constants so that κ is dimensionless and K has the dimension $(\text{length})^{-2}$.

[30] M. Goulian, N. Lei, J. Miller, and S.K. Sinha, Phys. Rev. A **46**, R6170 (1992).